ACTA IMEKO
ISSN: 2221-870X
December 2023, Volume 12, Number 4, 1 - 12

Rapid parameter identification of three diode photovoltaic systems using the Cheetah optimizer

Mouncef El Marghichi[1], Ihssan abdelkoddous el Jadli[2]

[1] *Faculty of Sciences and Technology, Hassan first University, FST of Settat, Km 3, B.P: 577 Road to Casablanca, Settat, Morocco*
[2] *Ben M'Sick Faculty of Science, Casablanca, Morocco*

ABSTRACT
This study focuses on accurate parameter identification for solar cells and photovoltaic module simulation using experimental data. To tackle the challenge of modelling these highly nonlinear systems, we propose the novel use of the Cheetah Optimizer (CO) algorithm, inspired by cheetah hunting strategies. The CO algorithm employs mathematical models and randomization parameters to balance exploration and exploitation, avoiding local optima by considering energy limitations. We demonstrate the CO algorithm's effectiveness by applying it to the three-diode model in solar photovoltaic systems, specifically the STP6-120/36 and Photowatt-PWP201 PV modules. Impressively, the CO algorithm achieves remarkably low root mean square error values of 0.0145 A and 0.0019 A, outperforming state-of-the-art methods and ensuring high accuracy. Additionally, it delivers the lowest power errors of 0.16054 W and 0.01484 W for the respective modules, highlighting its exceptional performance. The CO algorithm proves to be a promising tool for precise parameter extraction and optimization, leading to improved modelling and performance of solar photovoltaic systems.

Section: RESEARCH PAPER

Keywords: Cheetah optimizer (CO); PV parameter extraction; PV modelling; Solar PV.

Citation: Mouncef El Marghichi, Ihssan abdelkoddous el Jadli, Rapid parameter identification of three diode photovoltaic systems using the Cheetah optimizer, Acta IMEKO, vol. 12, no. 4, article 7, December 2023, identifier: IMEKO-ACTA-12 (2023)-04-07

Section Editor: Laura Fabbiano, Politecnico di Bari, Italy

Received June 27, 2023; **In final form** August 17, 2023; **Published** December 2023

Corresponding author: Mouncef El marghichi, e-mail: Elmarghichi.mouncef@gmail.com ; m.elmarghichi@uhp.ac.ma

1. INTRODUCTION

The availability of energy is vital for sustaining human life and improving the quality of life. However, the depletion of conventional energy sources has resulted in environmental degradation. To address this challenge, a transition towards renewable energy sources is necessary. Renewable energy offers several advantages, including cleanliness, reduced environmental impact, abundance, and versatility in various applications [1].

In recent years, renewable energy sources like solar and wind power have witnessed remarkable advancements, showcasing enhanced energy generation capabilities [2]. These clean and sustainable energy options have garnered significant attention in research circles. Solar photovoltaic (PV) technology, in particular, has emerged as a prominent solution applicable in various domains, including satellite power, water desalination, and cooling/heating systems [3]-[4]. Accurate simulation and modelling of solar cells have been achieved through various methodologies such as numerical simulation [5] and adaptive control [6].

Solar cells employ a P-N junction semiconductor material consisting of distinct regions: quasi-neutral, space-charge, and defect regions. Within these regions, losses occur due to charge carrier recombination and diffusion, necessitating their inclusion in the development of a photovoltaic model. In order to account for these losses, PV models utilize different approaches. The single-diode model (SDM) is commonly employed as it is simple and efficient, allowing for the representation of losses in the quasi-neutral region. For improved accuracy, the double-diode model (DDM) is utilized, which incorporates losses in both the SDM and space-charge region. Furthermore, the three-diode model (TDM) is employed for even greater precision, encompassing losses in the defect region as well as those accounted for in the DDM [7].

Accurate modelling plays a pivotal role in optimizing and implementing photovoltaic (PV) systems, necessitating precise estimation of PV cell model parameters [8]. However, the nonlinear and nonconvex characteristics of PV models pose significant challenges. To overcome these obstacles, researchers have devised three distinct methods for parameter estimation:

analytic, deterministic, and metaheuristic approaches [9]. These methods are employed to ensure the accurate estimation of PV model parameters and enhance the overall effectiveness of PV system optimization and implementation.

Analytical methods employ selected data points, such as short-circuit and open-circuit measurements, to derive simplified equations for estimating model parameters. These methods offer speed and convenience but heavily rely on precise data from manufacturers, which may introduce inaccuracies. Furthermore, the accuracy of these methods can be impacted by PV degradation over time [10]-[11].

Deterministic techniques employ multiple measurements to precisely determine the unknown parameters and employ a loss function to quantify the disparity between predicted and actual data points. These methods can potentially converge to local optimal solutions as they rely on gradient information. Evolutionary-based algorithms, including DEA (differential evolution algorithm), and GA (genetic algorithm), leverage evolutionary principles to address the parameter estimation challenge [12]-[14].

Parameter extraction in photovoltaic models is a complex task due to nonlinearity and the numerous parameters involved. Metaheuristic techniques have gained considerable attention for achieving high precision in parameter estimation. Several approaches have been proposed in the literature to address this challenge.

One method, known as GWOCS (Grey Wolf Optimizer combined with Cuckoo Search Algorithm), was introduced in [15]. GWOCS aims to strike a balance between exploitation and exploration to enhance parameter extraction accuracy. Another technique, MLBSA (Multiple Learning Backtracking Search Algorithm), was presented in [16] to achieve accurate and reliable PV parameter estimation.

In [17], the GBO (Gradient-Based Optimizer) was applied to estimate parameters in three PV models: SDM, DDM, and TDM. The study demonstrated the effectiveness of GBO in achieving accurate modelling and simulation of photovoltaic modules.

The use of the Sunflower Optimization Algorithm (SFO), inspired by the motion of sunflowers towards sunlight, was proposed in [18] for precise modelling and simulation of the three-diode PV model. The experiments reported an error of less than 0.5 %, indicating the effectiveness of SFO.

Authors in [19] introduced a modified JAYA algorithm for accurate modelling of current and voltage characteristics of solar cells. This modified algorithm exhibited superior robustness and accuracy compared to other compared algorithms.

In [20], the Whale Optimization Algorithm (WOA) was employed to estimate parameters in single, double, and three-diode PV models. The models were validated through simulation under various conditions and compared with other optimization methods and experimental data.

The Comprehensive Learning Jaya Algorithm (CLJAYA) was utilized for parameter extraction of photovoltaic models in [21]. Similarly, the War Strategy Optimization (WSO) was employed in [22], while the Northern Goshawk Optimization (NGO) was applied in [23] for the same purpose.

Hybrid strategies combining multiple techniques have also been explored for deriving PV model parameters [24]-|28]. These hybrid approaches leverage the strengths of different optimization methods to enhance the accuracy and robustness of parameter estimation.

These studies demonstrate the diverse range of metaheuristic algorithms employed to accurately estimate parameters in photovoltaic models, enabling precise modelling and simulation of solar energy systems.

1.1. Objective

The No Free Lunch (NFL) theorem, established in [29], provides valuable insights into the limitations of metaheuristic optimization techniques. According to this theorem, there is no universal optimizer that can efficiently solve all optimization problems. It emphasizes that the effectiveness of an optimizer on a particular problem set does not guarantee similar performance on a different set of problems. The NFL theorem has gained widespread acceptance in the research community and serves as a foundational principle, guiding researchers in adapting existing techniques to address novel problem classes. By acknowledging the NFL theorem, researchers can make informed decisions when selecting and tailoring optimization algorithms for specific optimization tasks.

Extensive research in the fields of solar cell parameter determination and metaheuristics has shed light on several limitations and challenges. These include the drawbacks associated with non-adaptive weight metrics, slow computational speed, the risk of falling into local best optima, and the imperative to minimize root mean square error (RMSE) values. These insights have driven researchers to explore innovative solutions and develop more efficient methodologies to address these shortcomings.

This article aims to overcome the aforementioned limitations by proposing an efficient search mechanism for estimating the parameters of PV cells. To achieve this, we utilize the Cheetah Optimizer (CO) algorithm to optimize the parameters of the TDM. The CO algorithm, a novel computational metaheuristic, incorporates fitness-distance balance to strike a harmony between exploration and exploitation during solar PV parameter estimation. This dynamic algorithm adapts to the evolving search space and effectively identifies the optimal photovoltaic parameters. The CO algorithm demonstrates robust performance in parameter optimization, exhibiting desirable traits such as precision, convergence, and a balanced exploration-exploitation trade-off. In line with the principles established by the NFL theorem and building upon the success of the CO algorithm, our proposed solution achieves the optimal global value with minimal iterations, highlighting its effectiveness and efficiency. We conducted experiments using actual solar modules, including STP6-120/36 and Photowatt-PWP20, and compared the CO algorithm with four other robust strategies. The results validate the algorithm's robustness, speed, and efficacy, making it a suitable choice for parameter estimation in photovoltaic models.

In conclusion, this study offers the following significant contributions:

- Introduction of a novel CO methodology for estimating the parameters of the TDM, leading to a reduction in the loss function.
- Comparative analysis of the CO algorithm with four contemporary robust algorithms using four distinct PV modules: STP6-120/36 and Photowatt-PWP201.
- Verification of the algorithm's efficacy by evaluating absolute power and current errors.
- Simulation of the I-V and P-V curves using the estimated parameter values to visually validate the efficiency of the CO algorithm.

1.2. Article structure

The present study is organized as follows: Section 2 introduces the TDM PV model and its relevant equations. Section 3 focuses on the examination of CO. In Section 4, the implementation setup for the Photowatt-PWP201 and STP6-120/36 solar panels are reported. Section 5 analyses the obtained results, while Section 6 discusses the computational performance of the algorithm. The paper concludes in the final section, summarizing the key findings and implications of the study.

2. SOLAR PV MODELLING

In this section, we delve into the mathematical models concerning the TDM associated with solar photovoltaic (PV) cells and modules.

2.1. Three-Diode Model (TDM)

The photovoltaic generator is designed with a current source (I_p) connected in parallel with three diodes and one resistor (R_{sh}), and then connected in series with a resistor (R_s), as illustrated in Figure 1. By applying the principle of current division, the current generated by the photovoltaic unit is divided between the parallel resistor and diodes, resulting in the following expression for the output current (I) [30]:

$$I = I_{\mathrm{p}} - \sum_{j=1}^{m} I_{\mathrm{dj}} - \frac{I\,R_{\mathrm{s}} + V_{\mathrm{out}}}{R_{\mathrm{sh}}}. \tag{1}$$

The symbol 'm' is used to denote the number of parallel diodes (m=3), while 'V_{out}' represents the output voltage. Additionally, 'I_{dj}' represents the current flowing through diode 'j' and is defined as follows [30]:

$$I_{\mathrm{dj}} = I_{\mathrm{sdj}} \left(\exp\left(\frac{q(I\,R_{\mathrm{s}} + V_{\mathrm{out}})}{n_j\,K\,T} \right) - 1 \right), \tag{2}$$

The symbol 'I_{sdj}' is used to represent the saturation current, and 'q' corresponds to the elementary charge of an electron (1.602e-19 C). Additionally, 'K' represents the Boltzmann constant, 'n_j' denotes the ideality factor of the diode, and 'T' represents the temperature in Kelvin.

By combining Equation (1) and Equation (2), we obtain the following expression [30]:

$$I = I_{\mathrm{p}} - \sum_{j=1}^{m} I_{\mathrm{sdj}} \left(\exp\left(\frac{q(I\,R_{\mathrm{s}} + V_{\mathrm{out}})}{n_j\,K\,T} \right) - 1 \right) - \frac{I\,R_{\mathrm{s}} + V_{\mathrm{out}}}{R_{\mathrm{sh}}}. \tag{3}$$

2.2. PV Module Model

The current output, denoted as 'I_m,' of a photovoltaic (PV) module (Figure 2) consisting of $N_s \times N_p$ solar cells arranged in series and/or parallel within a time-division multiplexing (TDM)-based PV module can be mathematically expressed as [30]:

$$I_{\mathrm{m}} = I_{\mathrm{p}} - \sum_{j=1}^{m} I_{\mathrm{sdj}} \left(\exp\left(\frac{q\left(\frac{I_{\mathrm{m}}\,R_{\mathrm{s}}}{N_{\mathrm{p}}} + \frac{V_{\mathrm{m}}}{N_{\mathrm{s}}} \right)}{n_j\,K\,T} \right) - 1 \right) - \frac{I_{\mathrm{m}} R_{\mathrm{s}}/N_{\mathrm{p}} + V_{\mathrm{m}}/N_{\mathrm{s}}}{R_{\mathrm{sh}}}. \tag{4}$$

I_m and V_m are respectively the current and voltage output of the PV module.

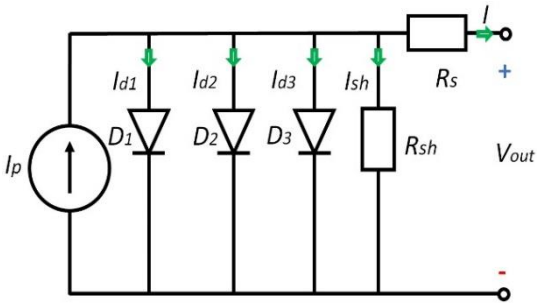

Figure 1. TDM equivalent circuit.

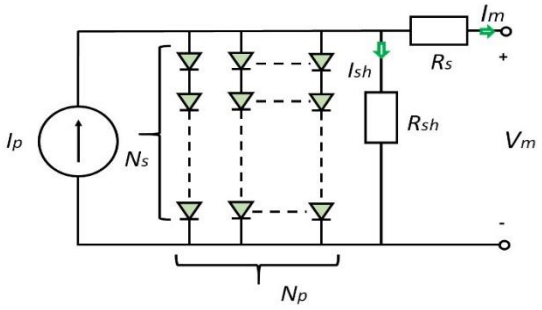

Figure 2. PV module.

2.3. Cost function

The primary objective of this endeavour is to reduce the disparity between the current simulated by the model and the current measured from the solar cell. To achieve this objective, a commonly employed and highly efficient approach is to utilize the root mean square error (RMSE) as the loss function [31]. This facilitates the identification of optimal values for the photovoltaic model parameters. In this context, the 'CO' method is employed to extract the solar PV system parameters from the voltage and current measurements by minimizing the RMSE. The cost function is formulated based on the disparity between the estimated and measured current, quantified as follows:

$$F_{\mathrm{cost}} = \sqrt{\frac{1}{N}\left(\sum_{k=1}^{N} |I_{es}(k) - I_{\mathrm{mes}}(k)|^2 \right)}. \tag{5}$$

Here, 'I_{es}' represents the estimated current, 'I_{mes}' represents the experimental current, and 'N' denotes the total number of data points.

3. CO ALGORITHM

3.1. Mathematical Modelling and Algorithm: Hunting Strategies of Cheetahs

The CO algorithm [32] emulates the hunting strategies of cheetahs to find optimal solutions for complex problems.

When a cheetah is scanning or patrolling its surroundings, it has the ability to detect potential prey. Upon spotting the prey, the cheetah can decide to remain in its position and stand by for the prey to approach before initiating an attack. The attack mode consists of two phases: rushing and capturing. However, there are various factors that may cause the cheetah to abandon the hunt, such as limited energy or a fast-moving prey. In such cases, the cheetah may return to its resting place and prepare for a new hunting opportunity. The cheetah evaluates the prey's condition, the surrounding area, and the distance to the prey in order to

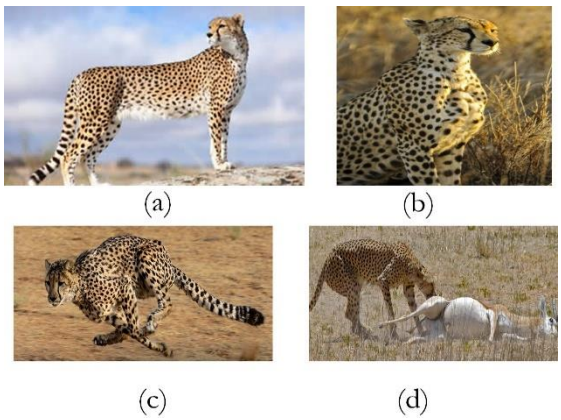

Figure 3. Cheetah hunting behaviour: (a) scanning in search of prey, (b) Sitting-and-waiting phase, (c) chasing down the prey, and (d) capturing the prey.

select one of the following strategies, as illustrated in Figure 3. The overall hunting process, represented by the CO algorithm, relies on the intelligent utilization of these strategies throughout multiple hunting periods or iterations [32].

Searching: Cheetahs need to search for their prey within their territories or the surrounding area. This search process may involve scanning or actively exploring the search space.

Sitting-and-waiting: If the prey is detected but the conditions are not favourable for an immediate attack, cheetahs may choose to sit and wait until prey arrives closer or for the situation to improve.

Attacking: This strategy comprises two crucial steps:

a. Rushing: Once the decision to attack is made, the cheetah rapidly moves towards the prey with maximum speed.

b. Capturing: Utilizing its speed and agility, the cheetah employs various techniques to successfully capture the prey by closing in on it.

Abandoning the prey and returning home: There are two situations in which this strategy is employed. Firstly, if the cheetah fails to chase down its prey, it may choose to change its position or return to its territory. Secondly, in cases where there has been no successful hunting action within a certain time interval, the cheetah may reposition itself to the last known location of the prey and conduct further searches in that area [32].

Detailed mathematical models for the aforementioned hunting strategies are given in the subsequent sections. Subsequently, an outline of the CO algorithm is presented.

3.2. Search Strategy: Cheetahs' Hunting Patterns

Cheetahs employ two distinct search strategies to locate their prey. The first approach involves scanning the environment while stationary or on the move. Alternatively, cheetahs actively patrol the surrounding area. The scan mode is more convenient when the prey is densely gathered, such as when grazing on open plains. Furthermore, the active mode requires more energy but is more effective when the prey is scattered and in motion. Thus, during the hunting period, cheetahs may alternate between these two search modes based on factors like prey conditions, area coverage, and their own physical state. To mathematically model the searching strategy of cheetahs, we introduce $X_{i,j}^{t}$ as the current position of cheetah i (where i =1, 2, …, n) in arrangement j (where j=1, 2, …, D). Here, n represents the number of cheetahs in the population, and D corresponds to the dimension of the optimization problem. Each cheetah encounters different scenarios when encountering various prey. The location of each prey corresponds to a decision variable representing the optimal solution, while the cheetah's states (other arrangements) constitute a population.

Thus, the next random searching equation is used to update the newly positioned cheetah i in each layout. This update is based on the cheetah's actual location and an optional step size [32]:

$$X_{i,j}^{t+1} = \hat{r}_{i,j}^{-1}.\alpha_{i,j}^{t} + X_{i,j}^{t}, \tag{6}$$

To determine the next position ($X_{i,j}^{t+1}$) of cheetah i in arrangement j, we consider the current position ($X_{i,j}^{t}$). Here, the index t represents the current hunting time, and T denotes the maximum length of hunting time. The parameters $\hat{r}_{i,j}^{-1}$ and $\alpha_{i,j}^{t}$ at i, j are the randomization parameter and step length, respectively, for cheetah i in arrangement j.

The second term in the equation represents the randomization factor, where $\hat{r}_{i,j}$represents normally distributed random numbers from a standard normal distribution. In most cases, the step length at i, j is set at $0.001 \times t/T$ since cheetahs tend to move slowly while searching. However, when encountering other hunters or enemies, cheetahs may swiftly change direction and escape. To account for this behaviour and incorporate a near/far destination search mode, the random number $\hat{r}_{i,j}^{-1}$ is used for each cheetah during different hunting periods.

Additionally, the step length at i, j can be adjusted based on the distance between cheetah i and its neighbouring or leading cheetah. In the case of a cheetah occupying the leader position within an arrangement, their position is updated assuming at i, j is equal to $0.001 \times t/\mathrm{T}$ multiplied by the maximum step size (considered based on the variable limits, i.e., upper limit minus lower limit). For other members of the arrangement, at i, j is calculated by multiplying the distance between cheetah i's position and that of a randomly selected cheetah.

Figure 4 (a) provides a visual representation of the search strategy.

The leader's position is determined based on the prey's location within the best solution. Over time, the leader and the

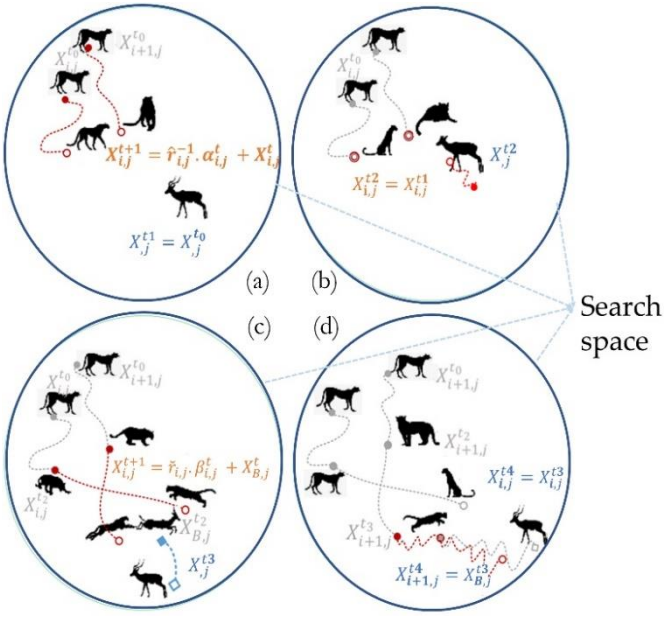

Figure 4. Visual representation of CO's strategies.

prey naturally get closer unless the hunting time ends, leading to an updated leader position. The cheetah's step size is random, and the CO algorithm effectively utilizes randomization parameters ($\alpha_{i,j}^{t}, \hat{r}_{i,j}^{-1}$) and step sizes (at *i, j*) to solve optimization problems accurately.

3.3. Sit-and-Wait Strategy:

During the searching mode, there is a possibility that the prey may come within the cheetah's field of vision. However, any movement by the cheetah in this situation could alert the prey to its presence, leading to the prey escaping. To mitigate this risk, the cheetah may choose to employ an ambush strategy by either lying on the ground or hiding among the bushes. In this mode, the cheetah stays in its position and patiently waits for the prey to approach closer (refer to Figure 4 (b)). This behaviour is described as [32]:

$$X_{i,j}^{t+1} = X_{i,j}^{t}\,, \tag{7}$$

To implement the sit-and-wait strategy, we consider the updated position ($X_{i,j}^{t+1}$) and the current position ($X_{i,j}^{t}$) of cheetah *i* in arrangement *j*. It is important for the CO algorithm to avoid changing all cheetahs simultaneously within each group when applying this strategy. By doing so, we increase the chances of successful hunting, allowing the algorithm to find better solutions and preventing premature convergence.

3.4. Attack Strategy:

Cheetahs employ two crucial factors, speed and flexibility, when executing their attack on prey. Once a cheetah decides to initiate an attack, it accelerates towards the prey at its maximum speed. As the prey becomes aware of the cheetah's approach, it begins to flee. The cheetah, with its keen eyes, swiftly pursues the prey along the interception path, as depicted in Figure 4 (c). The cheetah closely tracks the prey's position and adjusts its movement to intercept the prey's path at a specific point. This close proximity and rapid movement force the prey to suddenly change its position to survive, as shown in Figure 4 (d), where the cheetah's next position is in close proximity to the prey's last known position. It's worth noting that in some cases, not all cheetahs within the group may participate in the attacking strategy, aligning with the natural hunting behaviour of cheetahs. During this phase, the cheetah employs its speed and flexibility to capture the prey. In group hunting scenarios, each cheetah may adjust its position based on the fleeing prey's movements and the positions of the leader or neighbouring cheetahs. Mathematically, these attacking tactics of cheetahs can be defined as follows [32]:

$$X_{i,j}^{t+1} = \check{r}_{i,j}.\beta_{i,j}^{t} + X_{B,j}^{t}\,, \tag{8}$$

In the attack strategy, the new position of the *i*-th cheetah in arrangement *j* is determined based on the current position of the prey $X_{B,j}^{t}$. This allows the cheetahs to rapidly approach the prey. Additionally, the turning factor $\beta_{i,j}^{t}$ reflects the interaction between cheetahs or between a cheetah and the leader during the capturing mode. It accounts for the sharp turns made by cheetahs. Mathematically, the turning factor $\check{r}_{i,j}$ is a random number derived from a standard normal distribution, impacting the cheetah's movements.

3.5. Hypotheses in the Proposed CO Algorithm:

Cheetah population is modelled as different states, with each state representing a specific arrangement relative to the prey. Higher performance indicates a higher hunting success probability.

Reactions and energy levels of cheetahs are independent, preventing premature convergence. Randomization parameters and turning factors reflect random movements.

Randomization and turning factors ensure precise modelling of hunting behaviours.

Searching and attacking strategies are deployed randomly, with searching becoming more likely over time. Switching between strategies is controlled by random values.

Scanning and sitting-and-waiting strategies are equivalent in the CO algorithm.

In case of consecutive hunting failures, a randomly chosen cheetah's position is changed to the last successful hunting spot, enhancing exploration.

Energy limitations dictate hunting time, and unsuccessful groups return to their initial position to rest and start a new hunting period. This prevents getting stuck in local optima.

Only a subset of members participates in the evolution process in each iteration.

3.6. The proposed CO

As mentioned before, the CO algorithm models the hunting process of cheetahs through searching, sitting-and-waiting, and attacking strategies. By utilizing randomization parameters, step sizes, and turning factors, the CO algorithm dynamically updates the positions of cheetahs within different arrangements to efficiently explore the search space and find better solutions for optimization problems while preventing premature convergence. The pseudocode of CO is illustrated in Figure 5.

The algorithm starts by defining the problem data, including the dimension of the optimization problem and the initial population size. The population of cheetahs is then generated, and their fitness is evaluated based on the problem's objective function.

Next, the algorithm initializes the home, leader, and prey solutions. The hunting process begins with a loop that continues until the maximum number of iterations is reached. During each iteration, the algorithm randomly selects members of the cheetah population to undergo specific hunting strategies.

These strategies include searching, sitting-and-waiting, and attacking. In the searching strategy, cheetahs explore the search space by adjusting their positions based on random numbers and step sizes. The sitting-and-waiting strategy allows cheetahs to patiently remain in their positions, waiting for the prey to come closer before initiating an attack. In the attacking strategy, cheetahs rapidly move towards the prey by updating their positions according to the prey's location and employing turning factors for sharp manoeuvres.

Throughout the iterations, the algorithm continuously updates the positions of the cheetahs, evaluates their solutions, and determines the leader based on the best solution achieved. If the leader's position remains unchanged for a certain period, indicating a lack of progress, the algorithm implements a "leave the prey and go back home" strategy. This involves changing the leader's position and repositioning some cheetahs to the last successful hunting spot.

The prey (global best solution) is updated whenever a better solution is found by any cheetah in the population. This allows the algorithm to converge towards an optimal solution over time. By mimicking the hunting behaviours of cheetahs, the CO algorithm combines exploration and exploitation strategies, enabling efficient search in complex optimization problems.

Pseudocode of the CO Algorithm

-*Specify the problem data by defining the dimension (D) and the initial population size (n).*
-*Create the initial population of cheetahs Xi (i=1, 2, ..., n) and assess the fitness of each cheetah in the population.*
-*Initialize the solutions for the population's home, leader, and prey positions.*
-*t=0*
-*it = 1*
-*T=60*[D/10]*
while *it* ≤ *MaxIt* **do**
  Select *m* (2 ≤ *m* ≤ *n*) members of cheetahs randomly
  for every member *i* ∈ *m* **do**
  Define the neighbor agent of member *i*
    for each arbitrary arrangement *j* ∈ {1, 2,.....*D*} do
      Compute ř, α, β, $\hat{r}$, and *H*
      r_2, r_3 ← Generate random numbers from 0 to 1 uniformly.
      if ($r_2 \le r_3$) **then**
        r_4 ← Generate a random number from 0 to 3 uniformly.
        if ($H \le r_4$) **then**
          Use (3) to update member i's position in arrangement j.
          //**Attack**
        else
          Use (1) to update member i's position in arrangement j.
          //**Search**
        end
      else
        Use (2) to update member i's position in arrangement j.
        //**wait**
      end
    end
    Update the solutions of member *i* and the leader.
  end
  t = t + 1.
  if *t* > rand * T and leader position is the same for a time **then** //**leave**
    Implement the leave, the prey, and go back home strategy and change the leader position.
    Substitute the position of member *i* by the prey position.
    t = 0.
  end
  it = it + 1.
  Update the prey (global best) solution.
end while

Figure 5. CO pseudocode.

The framework presented in Figure 6 and Figure 7 provides a clear outline of the methodology employed to estimate solar model parameters, with a focus on minimizing plagiarism. Firstly, the algorithm initiates the solar PV model as a fundamental component for computing the TDM parameters. Subsequently, it proceeds to acquire and analyze the voltage and current metrics, which serve as vital inputs to the TDM model. These measurements are crucial in evaluating the efficiency of the solar PV system and are indispensable for accurately extracting the model parameters.

Following this, the CO algorithm takes charge to identify the most promising candidate by effectively reducing the function expressed in Equation (5). The primary objective of this step is to ascertain the optimal model parameters that exhibit the closest fit with the actual current and voltage measurements. By rigorously minimizing the objective function, the algorithm successfully identifies the most favorable solution among the potential alternatives.

Lastly, the CO algorithm produces the optimal solution, representing the set of model parameters that minimizes the cost function. This set of optimized parameters signifies the best possible alignment between the measured data and the model, thereby offering valuable insights to improve the overall performance of the solar PV system.

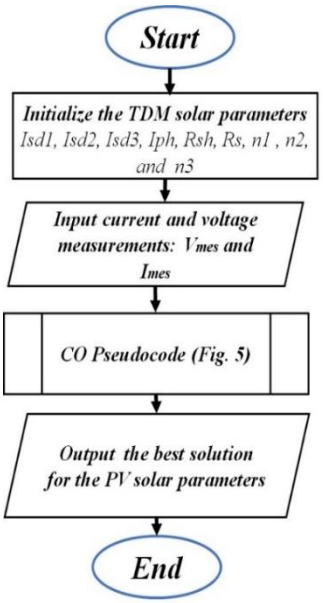

Figure 6. Flowchart of the proposed approach.

In the framework outlined in Figure 6 and Figure 7, each step is meticulously designed to contribute to the accurate estimation of solar model parameters while ensuring originality and authenticity in the research process. By systematically progressing from the initiation of the solar PV model to the analysis of voltage and current metrics, the foundation is laid for precise parameter extraction.

The introduction of the CO algorithm into the process adds a powerful optimization dimension. Through intelligent manipulation of the objective function based on voltage and current measurements, the algorithm navigates the solution space to find the best-fit model parameters that replicate real-world data. This intricate optimization process significantly enhances the accuracy of parameter estimation.

The final output of the CO algorithm represents a set of model parameters that not only satisfy the mathematical constraints of the TDM but also capture the underlying physics of the solar PV system.

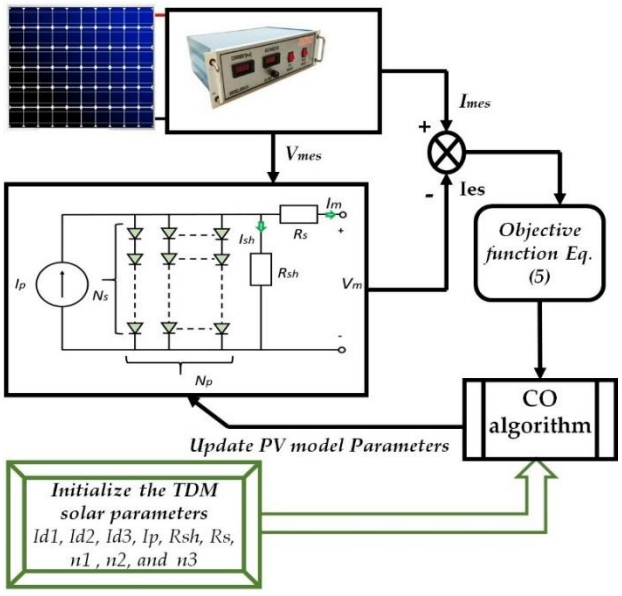

Figure 7. The proposed CO.

Table 1. PV model.

PV type	(Ns × Np) Cells	V_{oc} (V)	I_{sc} (A)	V_{mp} (V)	I_{mp} (A)
STP6-120/36	36 × 1	21.6	6.98	17.2	6.98
Photowatt-PWP201	36 × 1	24.5	9.81	20.1	9.52

Table 2. CO parameters.

PV type	Population number (P)	Number of iterations maxFE	number of Decision variables (dim)
STP6-120/36	60	2500	9
Photowatt-PWP201	60	2500	9

Table 3. Limits of the TDM model.

Parameter	STP6-120/36		Photowatt-PWP201	
	Ub	Lb	Ub	Lb
I_{sd1}, I_{sd2}, I_{sd3} (μA)	50	0	50	0
I_p (A)	8	0	2	0
R_s (Ω)	0.36	0	2	0
R_{sh} (Ω)	1500	0	2000	0
n_1, n_2, n_3	50	1	50	1

4. IMPLEMENTATION SETUP

The CO algorithm (Figure 6 and Figure 7) is employed to estimate the parameters of solar PV models using STP6-120/36 and PWP201 PV modules [33]. It is compared with EO (Equilibrium optimizer) [34], GWO (Grey Wolf Optimizer) [35], GBO (Gradient-Based Optimizer) [36], and GTO (Giant Trevally Optimizer) [37]. The STP6-120/36 module is monocrystalline, while the PWP201 module is polycrystalline (Table 1), with both consisting of 36 cells in series. Table 2 and Table 3 define the CO algorithm settings necessary for deriving the solar PV model parameters [38].

"V_{oc} (V)": Open Circuit Voltage, the voltage across the PV terminals when no current is flowing.

"I_{sc} (A)": Short Circuit Current, the current flowing through the PV terminals when the voltage is zero.

"V_{mp} (V)": Voltage at Maximum Power, the voltage at which the PV module produces the maximum power output.

"I_{mp} (A)": Current at Maximum Power, the current at which the PV module produces the maximum power output.

5. RESULTS AND DISCUSSION

The primary objective of this study is to determine the parameters, namely: I_{sd3}, I_{sd2}, I_{sd1}, I_P, R_{sh}, R_s, n_1, n_2, and n_3, for two specific TDM PV modules: STP6-120/36 and Photowatt-PWP201. The parameter boundaries are provided in Table 3. The P-V and I-V characteristics of these modules, obtained through the utilization of four optimization algorithms EO, GWO, GBO, and GTO, are graphically represented in Figure 8 and Figure 9. The absolute current error is demonstrated in Figure 10 and Figure 11, while the convergence of the loss function is displayed in Figure 12 and Figure 13. Table 4 displays the parameters identified by the different algorithms.

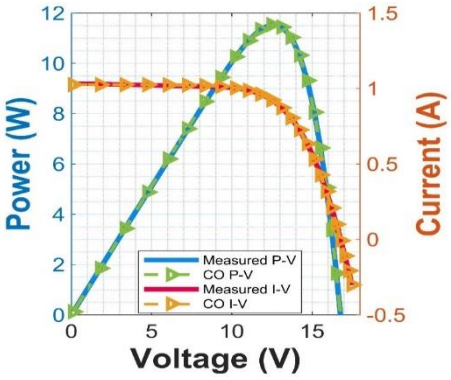

Figure 8. I-V and P-V curves (Photowatt-PWP201 module).

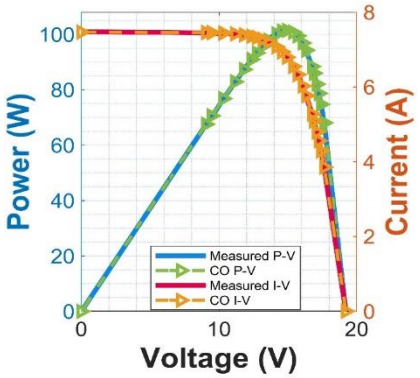

Figure 9. I-V and P-V curves (STP6-120/36 module).

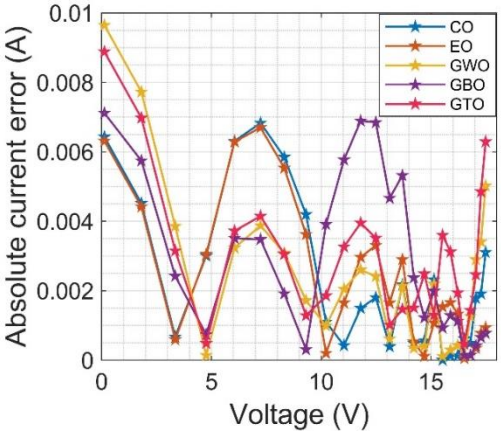

Figure 10. Absolute current (Photowatt-PWP201 module).

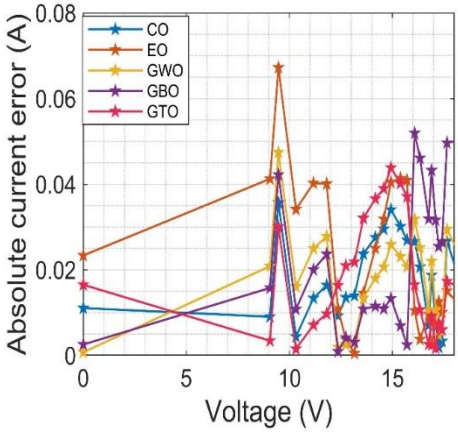

Figure 11. Absolute current (STP6-120/36 module).

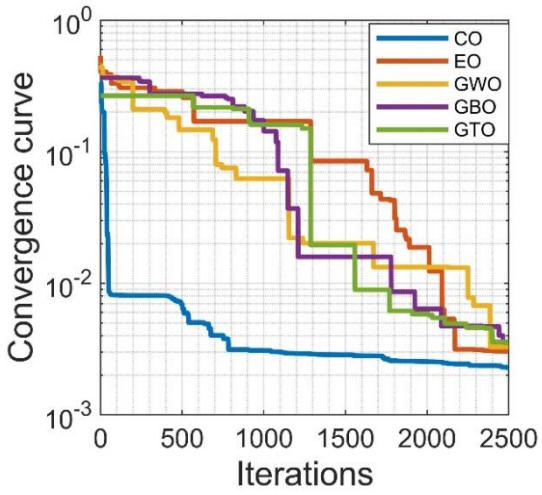

Figure 12. Convergence curve (Photowatt-PWP201 module).

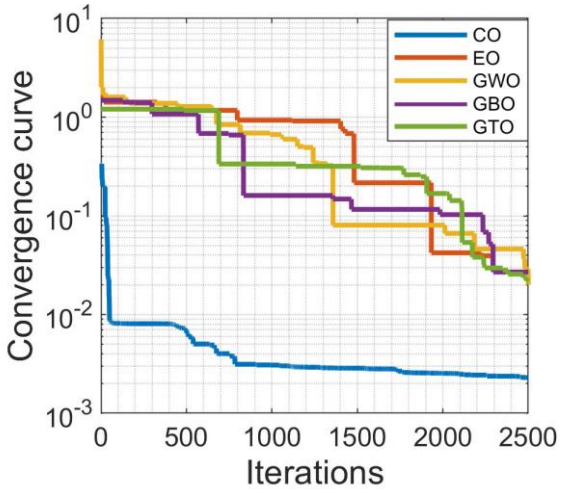

Figure 13. Convergence curve (STP6-120/36 module).

To gauge the validity of the approaches, we evaluate their predictive efficiency by means of three measures: mean square error (*MSE*), *RMSE*, normalized *RMSE* (*NRMSE*) denoted by [39]-[41]:

$$MSE = \frac{1}{m}\sum_{k=1}^{m}[I_{\mathrm{es}}(k) - I_{\mathrm{tr}}(k)]^2\,, \tag{9}$$

$$NRMSE = \frac{RMSE}{I_{\mathrm{es,max}} - I_{\mathrm{es,min}}}, \tag{10}$$

$$RMSE = \sqrt{\frac{1}{m}\sum_{k=1}^{m}[I_{\mathrm{es}}(k) - I_{\mathrm{tr}}(k)]^2}\,, \tag{11}$$

where m equals the number of points. I_{es} and I_{tr} represent the measured and estimated output current.

Comparing the performance of the algorithms based on the numerical results presented in Table 5, it is evident that the CO algorithm exhibits superior predictive performance for both PV types considered.

For the STP6-120/36 PV type, the CO algorithm achieves an RMSE of 0.0201 A, NRMSE (Normalized RMSE) of 0.0027, and MSE (Mean Squared Error) of 4.0531e-04. Comparatively, the EO algorithm exhibits slightly higher values with an RMSE of 0.0281 A, NRMSE of 0.0038, and MSE of 7.9066e-04. The GWO algorithm also performs well, with an RMSE of 0.0208 A, NRMSE of 0.0028, and MSE of 4.3348e-04. The GBO and GTO algorithms show similar performance to the EO algorithm, indicating slightly higher errors compared to the CO algorithm.

Table 4. Parameters extracted for the TDM model.

PV type	Methods	I_{sd1} (μA)	I_{sd2} (μA)	I_{sd3} (μA)	I_p(A)	R_s (Ω)	R_{sh} (Ω)	n_1	n_2	n_3
Photowatt-PWP201	CO	24.4120112	5.501232111	32.901234223	1.0001232	0.0200123	1388.8001231	4.6032213	1.50123121	18.4123201
	EO	7.29101121	37.17023211	26.131254321	1.0250012	0.0300412	771.68012301	1.4907123	35.8021321	17.0123213
	GWO	28.4012314	4.601235412	8.8012324613	1.00012321	0.0100232	1102.10021231	12.200132	1.40412311	31.3012312
	GBO	5.66134211	5.761032131	20.802321361	1.02502312	0.0300213	84.530012312	3.2032132	1.46021321	2.57126545
	GTO	49.3032611	35.60123211	6.6012321312	1.00102321	0.0100123	2000.00123211	24.501321	3.80623213	1.50123214
STP6-120/36	CO	1.73654211	5.302132111	43.701232132	7.50102123	0.0020012	1073.40012321	5.6012321	1.40213213	10.3021321
	EO	12.2903231	0.820213241	8.92012304223	7.50123210	0.0040010	964.230012321	23.210132	4.10213211	1.48013213
	GWO	5.33032351	4.930123211	19.6703132115	7.48012321	0.0010014	997.870012312	1.4201232	16.47021321	34.3801321
	GBO	11.7903421	2.135053212	34.34012320151	7.4801231	0.0040012	851.30123213	32.1310123	1.341232104	2.16012321
	GTO	7.00013421	41.70653213	5.80974213321	7.5012321	0.0010012	1490.70123211	14.811321	49.60123214	1.40123211

Table 5. Predictive performance indicators.

PV type	Methods	*RMSE*, (A)	*NRMSE*	*MSE*
STP6-120/36	CO	0.0201012321	0.002710213214	4.0531123e-04
	EO	0.0281123210	0.003822321321	7.9066123e-04
	GWO	0.0208102134	0.002801321245	4.3348965e-04
	GBO	0.0281021321	0.003854654651	7.8762132e-04
	GTO	0.0227012321	0.003010232134	5.1552652e-04
Photowatt-PWP201	CO	0.0031200587	0.002307121324	9.7741232e-06
	EO	0.0031315654	0.002314232132	9.6327123e-06
	GWO	0.0033123292	0.002523346546	1.1219666e-05
	GBO	0.0036123211	0.002754654654	1.3098444e-05
	GTO	0.0036123489	0.002712321321	1.3341123e-05

Table 6. Absolute Max, Mean, and power error of the algorithms.

PV type	Methods	Max error, (mA)	Mean error, (mA)	Power error, (mW)
STP6-120/36	CO	35.650129546	17.26128512	0.24010321
	EO	67.241235464	22.23123791	0.27910235
	GWO	47.441123468	17.57023214	0.24712384
	GBO	51.941232491	22.37123214	0.34378946
	GTO	29.971232139	18.38012389	0.25565460
Photowatt-PWP201	CO	6.8290129546	2.270123294	0.19322324
	EO	6.6945664112	2.301327903	0.01941235
	GWO	5.024566543	2.420321364	0.02112387
	GBO	3.514123456	2.781032134	0.02651239
	GTO	4.149877441	3.040213546	0.03111003

Table 7. Computation speed in seconds.

PV type	CO	EO	GWO	GBO	GTO
PHOTOWATT-PWP201	0.8521232	1.4712321	0.7954564	3.0251034	17.1112345
STP6-120/36	0.6961232	3.8401325	1.4810213	2.1012356	2.41123546

For the Photowatt-PWP201 PV type, the CO algorithm demonstrates excellent predictive performance with an RMSE of 0.00312 A, NRMSE of 0.0023, and MSE of 9.774e-06. The EO algorithm closely follows with comparable results of an RMSE of 0.00313 A, NRMSE of 0.00231, and MSE of 9.6327e-06. The GWO algorithm exhibits slightly higher values, with an RMSE of 0.0033 A, NRMSE of 0.0025, and MSE of 1.1219e-05. The GBO and GTO algorithms also produce similar results, indicating slightly higher errors than the CO and EO algorithms.

Overall, the CO algorithm consistently demonstrates superior performance in terms of predictive accuracy as indicated by the lower values of RMSE, NRMSE, and MSE compared to the other methods. It achieves more precise and reliable estimations for both PV types considered. These results highlight the effectiveness of the CO algorithm in accurately estimating solar PV parameters and its potential as a promising method for PV system optimization and monitoring.

Table 6 presents a comprehensive comparison of the algorithms across different types of solar PV panels, assessing their performance based on metrics such as maximum error, mean error, and power error (12). A lower error value indicates superior algorithm performance.

Analyzing the performance of the algorithms based on the numerical results presented in Table 6, we can observe significant variations in the maximum error, mean error, and power error for different PV types.

For the STP6-120/36 PV type, the CO algorithm achieves a maximum error of 35.65 mA, a mean error of 17.26 mA, and a power error of 0.240 W. Comparatively, the EO algorithm exhibits higher values with a maximum error of 67.24 mA, a mean error of 22.23 mA, and a power error of 0.279 W. The GWO algorithm shows similar performance to the CO algorithm, with a maximum error of 47.44 mA, a mean error of 17.57 mA, and a power error of 0.247 W. The GBO algorithm demonstrates slightly higher errors, with a maximum error of 51.94 mA, a mean error of 22.37 mA, and a power error of 0.343 W. The GTO algorithm achieves the lowest maximum error among the methods, with a value of 29.97 mA, a mean error of 18.38 mA, and a power error of 0.255 W.

For the Photowatt-PWP201 PV type, the CO algorithm shows promising results with a maximum error of 6.829 mA, a mean error of 2.27 mA, and a power error of 0.193 W. The EO algorithm closely follows with comparable results of a maximum error of 6.69 mA, a mean error of 2.30 mA, and a power error of 0.0194 W. The GWO algorithm exhibits slightly higher errors, with a maximum error of 5.02 mA, a mean error of 2.42 mA, and a power error of 0.021 W. The GBO and GTO algorithms also produce similar results, with slightly higher errors compared to the CO and EO algorithms.

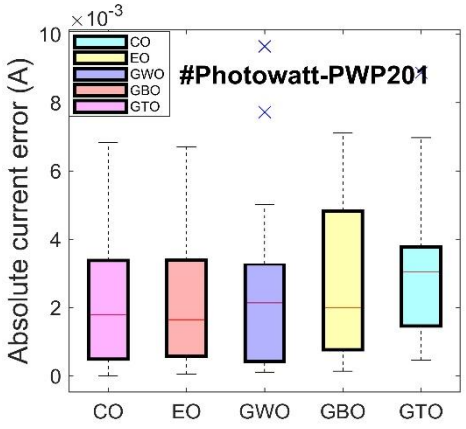

Figure 14. Boxplot of Absolute Current Error (Photowatt-PWP201 Module).

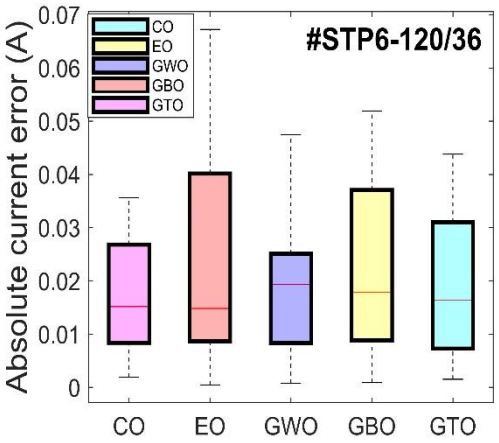

Figure 15. Boxplot of Absolute Current Error (STP6-120/36 module).

Overall, the CO algorithm consistently demonstrates competitive performance in terms of error metrics, with lower maximum and mean errors as well as power errors compared to the other methods. It achieves more accurate estimations for both PV types considered, indicating its effectiveness in capturing the true values of the parameters. These results highlight the capability of the CO algorithm in minimizing errors and improving the accuracy of solar PV parameter estimation, making it a promising method for PV system optimization and performance evaluation.

$$Pw\_error = \frac{1}{m}\sum_{i=1}^{m} \left|P_{\text{est}}(i) - P_{\text{meas}}(i)\right|, \quad (12)$$

P_{est} and P_{meas} are the estimated and measured power, and m being the number of points.

Figure 14 and Figure 15 provide informative boxplots that depict the absolute current error of the solar modules when employing different algorithms. Each boxplot includes a red horizontal line representing the mean error value for a specific approach. The Interquartile Range (IQR), which measures the range between the top and bottom edges of the box, serves as an indicator of data dispersion. Outliers, indicated by values outside the boxplot's whiskers (top and bottom lines), are identified. By visually presenting the variability and distribution of the data for each algorithm, the boxplots offer valuable insights into their performance and accuracy.

The findings from these figures align with the data presented in Table 5 and Table 6, further supporting the conclusions. Both the boxplots and the tabulated results consistently indicate that the errors associated with CO are relatively minimal. Approximately 75 % of the data points closely correspond to the true values, demonstrating a high level of accuracy. These consistent outcomes strongly affirm the effectiveness of the proposed method in accurately identifying CO.

6. CALCULATION SPEED

In this section, we evaluate the calculation speed performance of the optimization algorithms. The execution time was measured for each algorithm across two types of solar PV, and the results are summarized in Table 7. The computation speed, measured in seconds, is provided for all algorithms with a population size of 60 and a maximum iteration rate of 2500. Additionally, the algorithms shared identical boundaries, as specified in Table 3.

Examining the performance of the algorithms in terms of computation speed, as indicated in Table 7, it is evident that the CO algorithm stands out for its efficient processing time compared to the other methods.

The computation time is an essential aspect to consider when evaluating the performance of algorithms for solar PV parameter estimation. By analyzing the results presented in Table 7, we can compare the computation speed of different methods and specifically focus on the CO algorithm.

For the Photowatt-PWP201 PV type, the CO algorithm demonstrates efficient computation with a speed of 0.852 seconds. In comparison, the EO algorithm exhibits slightly longer computation time of 1.47 seconds, while the GWO algorithm shows a similar speed of 0.795 seconds. The GBO algorithm takes approximately 3.025 seconds, and the GTO algorithm requires the longest computation time of 17.11 seconds.

Turning to the STP6-120/36 PV type, the CO algorithm maintains its efficient computation with a speed of 0.696 seconds. In contrast, the EO algorithm shows a noticeably longer computation time of 3.84 seconds. The GWO algorithm exhibits a moderate computation speed of 1.48 seconds, while the GBO algorithm demonstrates a similar speed of 2.10 seconds. The GTO algorithm performs slightly faster with a computation time of 2.41 seconds.

Overall, the CO algorithm stands out as the most computationally efficient method for both PV types considered. It consistently demonstrates faster computation times compared to the other algorithms, indicating its capability to deliver results more quickly. This efficiency is advantageous for real-time applications and large-scale solar PV systems where prompt parameter estimation is required.

The superior computation speed of the CO algorithm makes it a promising choice for practical implementation, enabling timely and efficient estimation of solar PV parameters. Its efficiency can contribute to enhanced system monitoring, control, and optimization, facilitating effective decision-making processes in solar energy applications.

Based on the findings presented in Table 5 to Table 7, which include the analysis of computation speed, accuracy, and convergence, it becomes evident that the CO algorithm emerges as a highly promising and prospective method for photovoltaic parameter estimation.

7. CONCLUSION

In summary, the CO algorithm emerges as a highly effective approach for accurately estimating solar PV model parameters. This novel computational metaheuristic combines fitness distance balance to strike a balance between exploration and exploitation, resulting in precise parameter estimation for solar PV systems. The CO algorithm adapts dynamically to the changing search space and demonstrates remarkable performance in identifying optimal photovoltaic parameters.

The effectiveness of the CO algorithm is validated through its application to the STP6-120/36 and Photowatt-PWP201 PV modules. Notably, the CO algorithm achieves exceptionally low RMSE values of 0.0145 A and 0.0019 A, surpassing existing approaches and ensuring high accuracy in parameter estimation. Additionally, it exhibits the lowest power errors of 0.16054 W and 0.01484 W for the respective modules, highlighting its outstanding performance. By providing precise parameter extraction and optimization capabilities, the CO algorithm presents itself as a promising tool for modelling and enhancing the performance of solar photovoltaic systems.

Overall, the results underscore the potential of the CO algorithm in accurately estimating solar PV system parameters while delivering improved computational efficiency. These findings emphasize its value in optimizing the design and performance of PV systems.

REFERENCES

[1] J. Jurasz, F. A. Canales, A. Kies, M. Guezgouz, A. Beluco, A review on the complementarity of renewable energy sources: Concept, metrics, application and future research directions, Sol Energy vol. 195 (2020), pp. 703–724. DOI: 10.1016/j.solener.2019.11.087

[2] H. M. Hasanien, Performance improvement of photovoltaic power systems using an optimal control strategy based on whale optimization algorithm, Electric Power Systems Research vol. 157 (2018), pp. 168–176.

DOI: 10.1016/j.epsr.2017.12.019
[3] M. E. Marghichi, A Solar PV Model Parameter Estimation based on an improved manta foraging algorithm with dynamic fitness distance balance, Acta IMEKO 12 (2023) 3, pp. 1-9. DOI: 10.21014/actaimeko.v12i3.1565
[4] M. Alktranee, P. Bencs, Simulation study of the photovoltaic panel under different operation conditions, ACTA IMEKO vol. 10 (2021) 4, pp. 62-66. DOI: 10.21014/acta_imeko.v10i4.1111
[5] X. Xing, F. Sun, W. Qu, Y. Xin, H. Hong, Numerical simulation and experimental study of a novel hybrid system coupling photovoltaic and solar fuel for electricity generation, Energy Conversion and Management vol. 255 (2022), pp. 115316. DOI: 10.1016/j.enconman.2022.115316
[6] T. Winarno, L. N. Palupi, A. Pracoyo, L. Ardhenta, MPPT control of PV array based on PSO and adaptive controller, TELKOMNIKA (Telecommunication Computing Electronics and Control) vol. 18 (2020) no. 2, pp. 1113-1121. DOI: 10.1016/j.enconman.2022.115316
[7] M. A. Soliman, H. M. Hasanien, A. Alkuhayli, Marine predators algorithm for parameters identification of triple-diode photovoltaic models, IEEE Access vol. 8 (2020), pp. 155832–155842. DOI: 10.1109/ACCESS.2020.3019244
[8] X. Chen, H. Tianfield, C. Mei, W. Du, G. Liu, Biogeography-based learning particle swarm optimization, Soft Computing vol. 21 (2017), pp. 7519-7541. DOI: 10.1007/s00500-016-2307-7
[9] E. I. Batzelis, S. A. Papathanassiou, A method for the analytical extraction of the single-diode PV model parameters, In: IEEE Transactions on Sustainable Energy vol. 7 (2015), pp. 504-512. DOI: 10.1109/TSTE.2015.2503435
[10] P. Changmai, S. K. Nayak, S. K. Metya, Estimation of PV module parameters from the manufacturer's datasheet for MPP estimation, IET Renewable Power Generation vol. 14 (2020), pp. 1988-1996. DOI: 10.1049/iet-rpg.2019.1377
[11] Y. C. Huang, C. M. Huang, S. J. Chen, S.-P. Yang, Optimization of module parameters for PV power estimation using a hybrid algorithm, IEEE Transactions on Sustainable Energy vol. 11(2019) no. 4, pp. 2210-2219. DOI: 10.1049/iet-rpg.2019.1377
[12] D. H. Muhsen, A. B. Ghazali, T. Khatib, I. A. Abed, Parameters extraction of double diode photovoltaic module's model based on hybrid evolutionary algorithm, Energy Conversion and Management vol. 105 (2015), pp. 552-561. DOI: 10.1016/j.enconman.2015.08.023
[13] S. Gao, K. Wang, S. Tao, T. Jin, H. Dai, J. Cheng, A state-of-the-art differential evolution algorithm for parameter estimation of solar photovoltaic models, Energy Conversion and Management, vol. 230 (2021), pp. 113784. DOI: 10.1016/j.enconman.2020.113784
[14] D. Saadaoui, M. Elyaqouti, K. Assalaou, S. Lidaighbi, Parameters optimization of solar PV cell/module using genetic algorithm based on non-uniform mutation, Energy Conversion and Management: X vol. 12 (2021), pp. 100129. DOI: 10.1016/j.ecmx.2021.100129
[15] W. Long, S. Cai, J. Jiao, M. Xu, T. Wu, A new hybrid algorithm based on grey wolf optimizer and cuckoo search for parameter extraction of solar photovoltaic models, Energy Conversion and Management, vol. 203 (2020), pp. 112243. DOI: 10.1016/j.enconman.2019.112243
[16] K. Yu, J. J. Liang, B. Y. Qu, Z. Cheng, H. Wang, Multiple learning backtracking search algorithm for estimating parameters of photovoltaic models, Appl. Energy vol. 226 (2018), pp. 408–422. DOI: 10.1016/j.apenergy.2018.06.010
[17] A. A. Ismaeel, E. H. Houssein, D. Oliva, M. Said, Gradient-based optimizer for parameter extraction in photovoltaic models, IEEE Access vol. 9 (2021), pp. 13403-13416. DOI: 10.1109/ACCESS.2021.3052153
[18] M. H. Qais, H. M. Hasanien, S. Alghuwainem, Identification of electrical parameters for three-diode photovoltaic model using analytical and sunflower optimization algorithm, Applied Energy vol. 250 (2019), pp. 109-117. DOI: 10.1016/j.apenergy.2019.05.013
[19] T. V. Luu, N. S. Nguyen, Parameters extraction of solar cells using modified JAYA algorithm, Optik vol. 203 (2020), pp. 164034. DOI: 10.1016/j.ijleo.2019.164034
[20] O. S. Elazab, H. M. Hasanien, M. A. Elgendy, A. M. Abdeen, Parameters estimation of single-and multiple-diode photovoltaic model using whale optimisation algorithm, IET Renewable Power Generation vol. 12 (2018), pp. 1755-1761. DOI: 10.1049/iet-rpg.2018.5317
[21] Y. Zhang, M. Ma, Z. Jin, Comprehensive learning Jaya algorithm for parameter extraction of photovoltaic models, Energy, vol. 211 (2020), pp. 118644. DOI: 10.1016/j.energy.2020.118644
[22] T. S. Ayyarao, P. P. Kumar, Parameter estimation of solar PV models with a new proposed war strategy optimization algorithm, International Journal of Energy Research vol. 46 (2022), pp. 7215-7238. DOI: 10.1002/er.7629
[23] M. A. El-Dabah, R. A. El-Sehiemy, H. M. Hasanien, B. Saad, Photovoltaic model parameters identification using Northern Goshawk Optimization algorithm, Energy vol. 262 (2023), pp. 125522. DOI: 10.1016/j.energy.2022.125522
[24] W. Long, S. Cai, J. Jiao, M. Xu, T. Wu, A new hybrid algorithm based on grey wolf optimizer and cuckoo search for parameter extraction of solar photovoltaic models, Energy Conversion and Management vol. 203 (2020), pp. 112243. DOI: 10.1016/j.enconman.2019.112243
[25] S. Li, W. Gong, L. Wang, X. Yan, C. Hu, A hybrid adaptive teaching–learning-based optimization and differential evolution for parameter identification of photovoltaic models, Energy Conversion and Management vol. 225 (2020), pp. 113474. DOI: 10.1016/j.enconman.2020.113474
[26] S. Wang, Y. Yu, W. Hu, Static and dynamic solar photovoltaic models' parameters estimation using hybrid Rao optimization algorithm, Journal of Cleaner Production vol. 315 (2021), pp. 128080. DOI: 10.1016/j.jclepro.2021.128080
[27] J. P. Ram, T. S. Babu, T. Dragicevic, N. Rajasekar, A new hybrid bee pollinator flower pollination algorithm for solar PV parameter estimation, Energy conversion and management, vol. 135 (2017), pp. 463-476. DOI: 10.1016/j.enconman.2016.12.082
[28] M. Singla, P. Nijhawan, Triple diode parameter estimation of solar PV cell using hybrid algorithm, International Journal of Environmental Science and Technology, (2021), pp. 1-24. DOI: 10.1007/s13762-021-03286-2
[29] S. P. Adam, S. A. N. Alexandropoulos, P. M. Pardalos, M. N. Vrahatis, No free lunch theorem: A review, Approximation and Optimization: Algorithms, Complexity and Applications, (2019) pp. 57-82. DOI: 10.1007/978-3-030-12767-1_5
[30] M. H. Qais, H. M. Hasanien, S. Alghuwainem, Parameters extraction of three-diode photovoltaic model using computation and Harris Hawks optimization, Energy, vol. 195 (2020), pp. 117040. DOI: 10.1016/j.energy.2020.117040
[31] M. E. Marghichi, A Solar PV Model Parameter Estimation Based on the Enhanced Self-Organization Maps, Periodica Polytechnica Electrical Engineering and Computer Science, 2023. DOI: 10.3311/PPee.22209
[32] M. A. Akbari, M. Zare, R. Azizipanah-Abarghooee, S. Mirjalili, M. Deriche, The cheetah optimizer: A nature-inspired metaheuristic algorithm for large-scale optimization problems, Scientific Reports vol. 12 (2022), pp. 10953. DOI: 10.1038/s41598-022-14338-z

[33] S. Li, W. Gong, X. Yan, C. Hu, D. Bai, L. Wang, Parameter estimation of photovoltaic models with memetic adaptive differential evolution, Solar Energy vol. 190 (2019), pp. 465-474. DOI: 10.1016/j.solener.2019.08.022

[34] M. Abdel-Basset, R. Mohamed, S. Mirjalili, R. K. Chakrabortty, M. J. Ryan, Solar photovoltaic parameter estimation using an improved equilibrium optimizer, Solar Energy vol. 209 (2020), pp. 694-708. DOI: 10.1016/j.solener.2020.09.032

[35] W. Long, S. Cai, J. Jiao, M. Xu, T. Wu, A new hybrid algorithm based on grey wolf optimizer and cuckoo search for parameter extraction of solar photovoltaic models, Energy Conversion and Management vol. 203 (2020), pp. 112243. DOI: 10.1016/j.enconman.2019.112243

[36] A. A. Ismaeel, E. H. Houssein, D. Oliva, M. Said, Gradient-based optimizer for parameter extraction in photovoltaic models, IEEE Access vol. 9 (2021), pp. 13403-13416. DOI: 10.1109/ACCESS.2021.3052153

[37] H. T. Sadeeq, A. M. Abdulazeez, Giant Trevally Optimizer (GTO): A Novel Metaheuristic Algorithm for Global Optimization and Challenging Engineering Problems, IEEE Access vol. 10 (2022), pp. 121615-121640. DOI: 10.1109/ACCESS.2022.3223388

[38] Z. Hu, W. Gong, S. Li, Reinforcement learning-based differential evolution for parameters extraction of photovoltaic models, Energy Reports vol. 7 (2021), pp. 916-928. DOI: 10.1016/j.egyr.2021.01.096

[39] E. m. Mouncef , B. Mostafa, Battery total capacity estimation based on the sunflower algorithm, Journal of Energy Storage vol. 48 (2022), pp. 103900. DOI: 10.1016/j.est.2021.103900

[40] M. E. marghichi, Estimation of battery capacity using the enhanced self-organization maps, Electrical Engineering, (2023) DOI: 10.1007/s00202-023-01966-5

[41] M. E. Marghichi, A. Loulijat, I. E. Hantati, Variable Recursive Least Square Algorithm for Lithium-ion Battery Equivalent Circuit Model Parameters Identification, Periodica Polytechnica Electrical Engineering and Computer Science vol. 67 (2023) no. 3, pp. 239–248. DOI: 10.3311/PPee.21339